Journal of General Virology (2004), **85**, 119–130 DOI 10.1099/vir.0.19435-0

The CD2v protein of African swine fever virus interacts with the actin-binding adaptor protein SH3P7

P. C. Kay-Jackson,[1]† L. C. Goatley,[1] L. Cox,[1] J. E. Miskin,[1]‡ R. M. E. Parkhouse,[2] J. Wienands[3] and L. K. Dixon[1]

Correspondence
Linda Dixon
linda.dixon@bbsrc.ac.uk

[1]Institute for Animal Health, Pirbright Laboratory, Ash Road, Pirbright, Woking, Surrey GU24 0NF, UK

[2]Gulbenkian Institute of Science, Oeiras, Portugal

[3]Department of Biochemistry and Molecular Immunology, University of Bielefeld, D-33615 Bielefeld, Germany

The predicted extracellular domain of the CD2v protein of African swine fever virus (ASFV) shares significant similarity to that of the CD2 protein in T cells but has a unique cytoplasmic domain of unknown function. Here we have shown that CD2v is expressed as a glycoprotein of approximately 105 kDa in ASFV-infected cells. In the absence of an extracellular ligand, the majority of CD2v appears to localize to perinuclear membrane compartments. Furthermore, we have shown using the yeast two-hybrid system and by direct binding studies that the cytoplasmic tail of CD2v binds to the cytoplasmic adaptor protein SH3P7 (mAbp1, HIP55), which has been reported to be involved in diverse cellular functions such as vesicle transport and signal transduction. A cDNA clone encoding a variant form of SH3P7 could also be identified and was found to be expressed in a wide range of porcine tissues. Deletion mutagenesis identified proline-rich repeats of sequence PPPKPC in the ASFV CD2v protein to be necessary and sufficient for binding to the SH3 domain of SH3P7. In ASFV-infected cells, CD2v and SH3P7 co-localized in areas surrounding the perinuclear virus factories. These areas also stained with an antibody that recognizes a Golgi network protein, indicating that they contained membranes derived from the Golgi network. Our data provide a first molecular basis for the understanding of the immunomodulatory functions of CD2v in ASFV-infected animals.

Received 18 June 2003
Accepted 22 September 2003

INTRODUCTION

African swine fever is an important haemorrhagic disease of domestic pigs, caused by a large double-stranded DNA virus, African swine fever virus (ASFV), the only member of the family *Asfarviridae* (Dixon *et al.*, 2000). The genome is approximately 170 kbp long and is predicted to encode at least 150 proteins, including proteins involved in virus–host interactions important for virus survival and transmission (Dixon *et al.*, 1994; Yanez *et al.*, 1995; Yozawa *et al.*, 1994). For example, proteins related to IAP and Bcl2 inhibit apoptosis (Brun *et al.*, 1998; Nogal *et al.*, 2001; Revilla *et al.*, 1997) and the A238L protein inhibits activation of NFκB-dependent gene transcription (Powell *et al.*, 1996; Revilla *et al.*, 1998) and also inhibits calcineurin phosphatase activity and hence NFAT transcription factor activation (Miskin *et al.*, 1998, 2000).

The EP402R gene encodes a protein with similarity to the T-cell adhesion molecule CD2, termed CD2v. CD2v contains a signal peptide, a predicted transmembrane domain and a 147 amino acid cytoplasmic tail. CD2v causes erythrocyte haemadsorption around cells infected with certain ASFV strains and the adhesion of virions to erythrocytes, linked to ASFV dissemination within the host (Rodriguez *et al.*, 1993; Borca *et al.*, 1994). ASFV infection of cultured peripheral blood mononuclear cells reduces the mitogen-dependent proliferation of lymphocytes within this culture, which do not become infected. Deletion of the gene encoding CD2v abrogates this effect (Borca *et al.*, 1998).

Cellular CD2 participates in many inter- and intracellular signalling events (Selvaraj *et al.*, 1987; Bierer *et al.*, 1988). Proline-rich regions within its cytoplasmic tail interact with the adaptor protein CD2AP, which is involved in receptor

†Present address: Department of Cellular Biochemistry, Max Planck Institute for Biochemistry, D-82152 Martinsried, Germany.

‡Present address: Oxford Biomedica, Medawar Centre, Robert Robinson Avenue, The Oxford Science Park, Oxford OX4 4GA, UK.

patterning, cytoskeletal polarization, integrin-linked signalling complex formation and dynamic actin organization (Dustin *et al.*, 1998; Kirsch *et al.*, 1999).

SH3 domains occur in different types of protein including enzymes, proteins associated with the cytoskeleton and adaptor proteins. Their interactions with proline-rich motifs regulate many functions including enzyme activity, ligand targeting and complex nucleation (reviewed in Pawson & Schlessinger, 1993; Pawson, 1995; Mayer & Gupta, 1998).

In this report we demonstrate that CD2v binds to the adaptor protein SH3P7 (also named mAbp1 or HIP55). SH3P7 is the mammalian homologue of the yeast actin-binding protein Abp1. SH3P7 contains an SH3 domain, an actin depolymerization factor homology (ADF-H) domain (Lappalainen *et al.*, 1998) and two tyrosines, which are phosphorylated following T- and B-cell receptor stimulation (Larbolette *et al.*, 1999; Kessels *et al.*, 2000, 2001). SH3P7 is linked to endocytosis, vesicle trafficking through the Golgi and signal transduction (Warren *et al.*, 2002; Fucini *et al.*, 2002; Mise-Omata *et al.*, 2003; J. Wienands and others, unpublished results). We have shown that CD2v and SH3P7 co-localize around the virus factories of infected cells, in perinuclear regions derived from the Golgi network. The implications of these findings on the functions of SH3P7 and CD2v during ASFV infection are discussed.

METHODS

Yeast two-hybrid system analysis. The complete predicted cytoplasmic tail of CD2v from the Malawi LIL20/1 isolate of ASFV, encoding aa 221–375, was cloned into the pGBT9 vector (Clontech), referred to as pGBT9CD2vct. Deletion mutants CD2vi, CD2vii and CD2viii, encoding aa 221–342, 221–306 and 297–335, respectively, were also cloned into pGBT9. The fragments were amplified by PCR from pGBT9CD2vct using the following primers: 5′-CGCGAATTCGCAAGTATTTTATATCAATCATAAC-3′ and 5′-CCCCTCGAGTTATGATTCAGGTGGAGAACATGA-3′ (CD2v i); 5′-CGCGAATTCGCAAGTATTTTATATCAATCATAAC-3′ and 5′-CCCCTCGAGCACCGTTTGGGTAGGGGAGATGG-3′ (CD2vii); and 5′-GGAATTCCCACTCAATCCATCTC-3′ and 5′-CGGGATCCATTCAGATGAAGGAC-3′ (CD2viii), which contain *Eco*RI and *Xho*I sites (CD2vi and CD2vii) or *Eco*RI and *Bam*HI sites (CD2viii), and ligated into these sites in pGBT9. A panel of clones encoding SH3 domain-containing proteins was kindly provided by Lynn Wilson, Yamanouchi Research Institute, Oxford, UK. These encoded the p85 subunit of phosphatidylinositol-3-kinase, the Lck and Fyn kinases and the N- and C-terminal SH3 domains of NADPH oxidase. The p22-Phox cytochrome *b* subunit of NADPH oxidase was used as a control substrate.

Yeast strain Y190 was doubly transformed with pGBT9CD2vct and a porcine macrophage cDNA library in the pACT2 vector (Clontech) (Miskin *et al.*, 1998). Clones expressing interacting proteins were selected by *HIS3* and *lacZ* reporter gene assays, by growth in the absence of histidine and by filter lift assays for β-galactosidase expression. Colonies were transferred to nitrocellulose membranes and frozen in liquid nitrogen. The nitrocellulose was then placed on filter paper soaked in Z buffer (60 mM Na_2HPO_4, 40 mM NaH_2PO_4, 10 mM KCl, 1 mM $MgSO_4$, 0·27 % β-mercaptoethanol, 1 mg X-Gal ml^{-1}) and incubated at 30 °C. Positive colonies became blue. Plasmids were isolated from positive colonies and retransformed into yeast strain Y190 with pGBT9CD2vct or a control plasmid of the ASFV A238L gene in pGBT9 to confirm interactions.

Sequence analysis. Sequencing was carried out using a Pharmacia Biotech ALFexpress automatic sequencer, according to the manufacturer's instructions.

PCR. RNA was purified from tissues ground under liquid nitrogen using Trizol (Sigma), and poly(A)$^+$ RNA was extracted using the oligotex mRNA midi kit (Qiagen). RT-PCR was carried out using RT-PCR beads (Pharmacia) according to the manufacturer's instructions. Primers amplified either 270 bp of the unique sequence in clones SH3P7ii and SH3P7iii (primers 5′-GTTCCCTGTGGCGGGGCCAGGCTGTG-3′ and 5′-GCCCTGGGTAGTGGTCAACGTGTGCC-3′) or the C-terminal 400 bp of the SH3P7i clone (primers 5′-GGCAAGCTGAGGAGCCCCTCC-3′ and 5′-TTACTCAATGAGCTCCACGTAGTT-3′).

The Gene Racer Kit (Clontech) was used to amplify the 5′ end of the porcine SH3P7 gene using a primer from within the SH3P7 clone. A PCR product of ~900 bp was obtained and cloned into the pGEMT vector (Promega).

***In vitro* binding studies.** The complete predicted cytoplasmic tail of CD2v from the Malawi LIL20/1 isolate encoding amino acids 221–375 was amplified from plasmid pGBT9CD2vct using the primer pair 5′-CGGGATCCCGAAAAAGAAAAAAACATGTTGAA-3′ and 5′-CCGGAATTCTTAAATAATTCTATCTACGTG-3′ containing *Bam*HI and *Eco*RI sites and ligated into these sites in the pET21a(+) vector (Novagen) to give plasmid T7CD2vct. Expression of the T7-tagged protein in the BL21(DE3) strain of *E. coli* was induced with IPTG at 30 °C for 2 h. The protein was purified on T7-antibody agarose (Novagen), according to the manufacturer's instructions. The SH3P7ii insert was amplified from the pACT2SH3P7ii library clone using the primer pair 5′-CGGGATCCCGGCAAGCTGAGGAGCCCC-3′ and 5′-CGGAATTCGTCTTTACTCAATGAGCTCCAC-3′ containing *Bam*HI and *Eco*RI sites and ligated into these sites in the pGEX2TK vector to give plasmid GSTSH3P7ii. The full-length mouse SH3P7 cDNA was cloned in the pRP261 vector. These two SH3P7 proteins were expressed as glutathione *S*-transferase (GST) fusions in the BL21(DE3) strain of *E. coli*, at 30 °C, following induction with IPTG for 2 h. The fusion proteins were purified and eluted from glutathione–Sepharose (Pharmacia), according to the manufacturer's instructions.

The GST fusion proteins or GST, immobilized on glutathione–Sepharose, were incubated with purified T7–CD2vct for 2 h at 4 °C in 0·025 % NP-40 in PBS, then washed three times with 0·05 % deoxycholate, 0·5 % NP-40, 150 mM NaCl, 50 mM Tris/HCl, pH 7·5. Bound proteins were separated by SDS-PAGE, transferred to a nitrocellulose membrane and detected by Western blotting using a mouse monoclonal primary antibody to the T7 epitope (Novagen) diluted 1 : 10 000, followed by a horseradish peroxidase (HRP)-conjugated rabbit anti-mouse secondary antibody diluted 1 : 2000.

Cell cultures. Vero cells were cultured in Dulbecco's modified Eagle's medium containing 10 % FBS.

Immunofluorescence. A fragment containing the CD2v gene from the Malawi LIL20/1 isolate, with its stop codon removed and a 350 bp upstream sequence containing the promoter region, was amplified by PCR from clone LMw8 (Dixon, 1988). Primers used were 5′-ATAAAGCTTGGGATCATTATATGACATGTAAC-3′ (forward) and 5′-ATAGGATCCAATAATTCTATCTACGTGAATAAGCG-3′ (reverse). This fragment was cloned into the *Hin*dIII and *Bam*HI sites in the pcDNA3 vector (Clontech). A double-stranded oligonucleotide encoding the influenza virus haemagglutinin epitope tag

(HA) and including a 3′ stop codon, with upstream *Bam*HI and downstream *Xba*I sites, was cloned downstream and in frame with the CD2v gene. The oligonucleotides were 5′-ATAGGATCCATG-GCTTACCCATACGACGTACCAGACTACGCATCACTATGATCTA-GAATA-3′ and 5′-TATTCTAGATCAGTTTAGGACTTCTTCTGAT-ATTAGTTTTTGTTCCATGGATCCTAT-3′. This plasmid was called CD2vHA.

A plasmid containing the mouse SH3P7 gene as a 3′ fusion with the enhanced green fluorescent protein (EGFP) gene has previously been described (Larbolette *et al.*, 1999). This gene fusion was amplified by PCR incorporating *Bam*HI and *Xba*I sites at the 5′ and 3′ ends and cloned in the pGEM-T vector. A 47 bp double-stranded DNA oligonucleotide containing the ASFV VP72 promoter was inserted upstream as a *Bam*HI–*Sph* I fragment to give plasmid VP72GFPSH3P7.

These constructs were transformed into Vero cells using Lipofectin (Invitrogen) according to the manufacturer's instructions and cells were infected with the BA71V tissue-culture adapted strain of ASFV. At various times after infection, cells were fixed with 3 % paraformaldehyde in PBS and permeabilized with 0·1 % Triton X-100 in PBS for 15 min. CD2v was detected using a rabbit antibody against the HA epitope (Santa Cruz) diluted 1 : 200, followed by a goat anti-rabbit Alexa Fluor 568 secondary antibody (Molecular Probes) diluted 1 : 200. The virus capsid protein VP72 was detected using mouse monoclonal antibody 4H3 (Cobbold *et al.*, 1996) at a concentration of 1 : 10. Anti-mouse secondary antibodies labelled with Alexa Fluor 488 or 633 were used at a concentration of 1 : 200 to detect bound antibodies. Cell nuclei and virus factories were stained with 4,6-diamidino-2-phenylindole (DAPI) at 0·4 μg ml^{-1}. Cells were imaged on a Leica TCS NT confocal microscope. Labelling controls included omission of primary antibody and adjustment of confocal imaging parameters to avoid all risk of cross talk between fluorophores.

Analysis of protein glycosylation. Vero cells in six-well dishes were infected with the BA71V ASFV isolate and transfected with CD2vHA using Lipofectin (Invitrogen). Cells were incubated with or without tunicamycin (10 μg ml^{-1}) for 16 h and harvested in lysis buffer containing 0·2 % NP-40 (500 μl per well). Cell extracts from three wells were immunoprecipitated using 30 μl of a 50 % slurry of anti-HA beads (Roche) and the beads were washed three times in PBS. For endoglycosidase F (endo-F) digestions, immunoprecipitates were washed in 0·1 M Tris/HCl, pH 7·5, then resuspended in 50 μl 0·1 M Tris/HCl, pH 7·5, and 1 unit endo-F added. After overnight incubation at 37 °C, 50 μl 2× SDS sample buffer was added and samples were separated by SDS-PAGE followed by immunoblotting using an HRP-conjugated anti-HA antibody (1 : 800). Endoglycosidase H (endo-H) digestions were carried out similarly except that 0·1 M sodium citrate, pH 5·5, was used with 0·005 units of endo-H.

RESULTS

The CD2v protein is glycosylated

CD2v contains 15 predicted *N*-linked glycosylation sites in its extracellular domain, in contrast to cellular CD2 which contains three or four. Vero cells were infected with ASFV BA71V isolate and transfected with the CD2vHA plasmid, which expresses HA epitope-tagged CD2v under the control of its own promoter, with or without tunicamycin, an inhibitor of *N*-linked glycosylation. No expression of CD2vHA could be detected in uninfected cells transfected with this plasmid (data not shown), indicating that all the CD2vHA protein expression in infected cells was driven by the ASFV gene promoter. At 16 h post-infection, cells were harvested and CD2vHA immunoprecipitated with anti-HA-coupled agarose. Immunoprecipitates were separated by SDS-PAGE, blotted onto membranes and probed with HRP-coupled anti-HA antibodies. In the presence of tunicamycin, CD2vHA was close to its predicted molecular mass (~42 kDa) (Fig. 1C, lane 2). In the absence of tunicamycin, the majority of CD2vHA was ~100 kDa (Fig. 1C, lane 1), confirming that glycosyl groups are added to CD2v.

Glycosyl groups added within the endoplasmic reticulum are sensitive to digestion with endo-H, whereas complex groups added within the *trans*-Golgi network are insensitive to endo-H. The CD2vHA plasmid was transfected into Vero cells infected with the BA71V ASFV isolate. At 16 h post-transfection, CD2vHA was immunoprecipitated from cell extracts with anti-HA antisera and immunoprecipitates were digested with endo-H or endo-F. A proportion of the high molecular mass form of CD2vHA was resistant to digestion with endo-H (Fig. 1B, lane 2), but digestion with endo-F resulted in the disappearance of this form and appearance of a smaller band (Fig. 1A, lane 2). This shows that a proportion of CD2vHA is transported beyond the endoplasmic reticulum, at least to the Golgi network. Some CD2vHA reaches the cell surface, as it causes haemadsorption of red blood cells around cells infected with the Lille isolate of ASFV. This isolate lacks a functional CD2v protein and does not cause haemadsorption around untransfected cells (data not shown).

CD2v localizes near virus factories in ASFV-infected cells

To follow CD2v localization during ASFV infection, CD2vHA was expressed in ASFV-infected Vero cells. Cells were fixed at 4, 12, 16 and 20 h post-infection and CD2vHA (shown in red) was detected by indirect immunofluorescence using a rat monoclonal antibody against the HA epitope and a fluorescent-labelled goat anti-rat secondary antibody. CD2v is expressed late in infection and therefore no expression could be detected at 4 h. From 12 h post-infection, a punctate pattern was detectable around the virus factories (Fig. 2D and F).

Yeast two-hybrid screen

Our analysis of CD2v in ASFV-infected cells showed large amounts of the protein in the cytoplasm. We therefore decided to use the yeast two-hybrid system to identify host proteins that bind to the CD2v cytoplasmic tail, which contains several potential protein interaction motifs. A porcine macrophage cDNA library (Miskin *et al.*, 1998) was screened using the yeast two-hybrid system, with the CD2v cytoplasmic tail from the Malawi LIL20/1 isolate of ASFV as bait. Positive clones were identified by growth in the absence of histidine and β-galactosidase expression. Five clones encoded proteins containing SH3 domains; three were similar to the SH3P7 protein (U58884), termed SH3P7i, -ii and -ii, and two were similar to Grb2 (AF498925). To

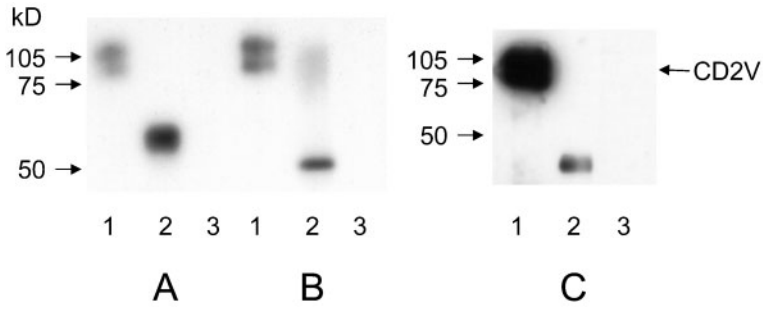

Fig. 1. Glycosylation of CD2v in ASFV-infected cells. Vero cells were infected with the BA71V ASFV isolate and transfected with a plasmid expressing the CD2v gene fused to the HA tag under the control of the CD2v gene promoter (lanes 1 and 2) or were mock transfected (lane 3). Cell extracts were harvested at 16 h post-infection. Cells used to prepare the extracts shown in lane 2 of (C) were incubated in the presence of tunicamycin (10 μg ml^{-1}). CD2vHA fusion proteins were purified by affinity chromatography using rat anti-HA antibodies coupled to agarose beads. Immunoprecipitates were untreated or digested with endoglycosidase F (A, lane 2) or endoglycosidase H (B, lane 2). Proteins were separated by SDS-PAGE, blotted onto Hybond C membrane and CD2vHA protein was detected by probing with rat anti-HA monoclonal followed by HRP-conjugated goat anti-rat antibodies. Bound proteins were detected by ECL. The positions of molecular mass markers run in parallel are shown.

confirm the specificity of the interactions, DNA was isolated from these clones and co-transformed into yeast with the CD2v bait plasmid or an irrelevant gene (ASFV A238L gene) in the bait vector. The interaction between the ASFV A238L protein and calcineurin was used as a positive control (Miskin *et al.*, 1998) (Table 1). β-Galactosidase expression and growth without histidine were used to confirm the interactions.

Proline-rich repeats in the CD2v cytoplasmic tail are necessary and sufficient for interaction with SH3P7

SH3 domains interact with sequences containing the consensus motif PXXP. The cytoplasmic tail of CD2v contains an area of repeats with the sequence KPCPPP, which seemed likely to interact with the SH3 domains. Truncated forms of the CD2v cytoplasmic tail, containing or lacking the proline repeats, were cloned into the yeast two-hybrid system bait vector. CD2vi encodes aa 221–342, from the predicted start of the cytoplasmic tail to the end of the proline repeats. CD2vii encodes aa 221–306, stopping before the repeats, and CD2viii encodes only the proline-rich region between aa 297 and 335 (see Fig. 3). The positive clones from the library screen were co-transformed into yeast with each truncation mutant and interactions were detected by growth in the absence of histidine and by assaying for β-galactosidase expression. The colour intensities in this assay were scored. A more intense colour resulted from an increased level of β-galactosidase expression, indicating a stronger interaction between the two proteins (Estojak *et al.*, 1995). The proline-rich repeats of CD2v were shown to be necessary and sufficient for its interactions with SH3 domains (Table 1). All positive interactions were with the complete cytoplasmic tail or with mutants encoding the proline-rich repeats, i.e. CD2vi and CD2viii. The strongest interactions were with two proteins with homology to SH3P7, i.e. SH3P7ii and SH3P7iii. These interactions were stronger than those with Grb2. The mutants were also used to screen a panel of SH3 domain-containing proteins to determine the specificity of the initial interactions. This panel contained the p85 subunit of phosphatidylinositol-3-kinase, the Lck and Fyn kinases and the N- and C-terminal SH3 domains of NADPH oxidase. The interaction between the NADPH oxidase SH3 domains and the NADPH cytochrome *b* domain, p22-Phox, was the positive control. None of this panel interacted with CD2v, strongly indicating that the interaction between CD2v and SH3P7 is specific (Table 1).

In vitro binding of CD2v with SH3P7 proteins

To confirm that CD2v and SH3P7 interact directly without requiring other proteins, binding studies were carried out using recombinant proteins. The CD2v cytoplasmic tail was expressed in *E. coli* with a T7 epitope tag in the pET 21a(+) vector (referred to as T7CD2vct). Following induction of expression, an additional 22 kDa band was detected by Western blotting with an anti-T7 antibody (Fig. 4A) and purified by affinity chromatography using anti-T7 antibody-coupled agarose. The SH3P7ii insert interacted most strongly with CD2v and so was cloned as a GST fusion in the pGEX2TK vector and referred to as GSTSH3P7ii. An additional 48 kDa band (Fig. 4B, lane 3) was detected following induction with IPTG and was purified using glutathione–Sepharose. The full-length mouse SH3P7 gene was also expressed as a GST fusion (GSTSH3P7) and the 80 kDa fusion protein purified by affinity chromatography (Fig. 4B, lane 2). Purified T7CD2vct was incubated with purified GSTSH3P7ii, GSTSH3P7 or GST immobilized on

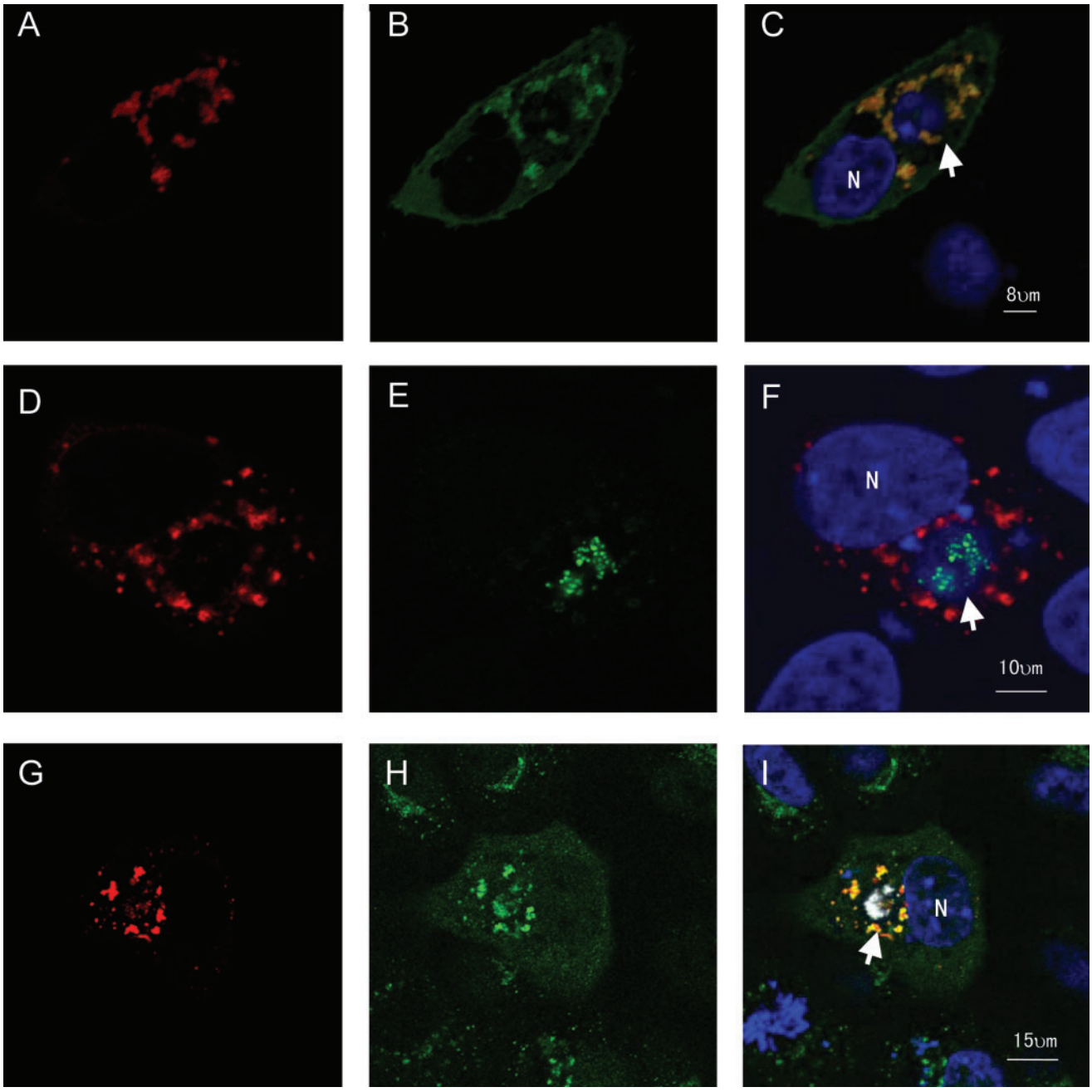

Fig. 2. Localization of CD2v and SH3P7 proteins in ASFV-infected cells. Vero cells were infected with the BA71V isolate of ASFV and transfected with a plasmid expressing the CD2v protein under the control of its own promoter fused to an HA epitope tag (A–I). A plasmid expressing the SH3P7 protein fused to the EGFP protein under the control of the ASFV VP72 promoter was co-transfected into cells (A–C). Cells were fixed at 18 h post-infection. The CD2v protein (red) was detected using a rat monoclonal antibody that recognizes the HA tag followed by Alexa 568-conjugated goat anti-rat antibodies (A, C, D, F, G and I). The EGFPSH3P7 fusion protein is shown in green (B). The overlaid images of (A) and (B) are shown in (C). (D) and (G) show infected cells that were transfected with the plasmid expressing CD2vHA alone (red). Virus factories were stained with a monoclonal antibody against the major capsid protein VP72 (E, green). (F) shows an image overlay of (D) and (E). The Golgi network was stained (green) with an antibody to the 103 kDa Golgi protein (H and I). (I) shows a overlay of (G) and (H) in which virus factories were also stained with a monoclonal antibody against the VP72 capsid protein (I, white). (C), (F) and (I) show DNA stained with DAPI (blue). Arrows indicate the position of virus factories and nuclei are labelled N.

Table 1. Interactions between CD2v deletion mutants and SH3 domain-containing proteins isolated from a porcine macrophage library and from a panel of SH3 domains

The complete cytoplasmic tail of CD2v (CD2vct) and deletion mutants of the cytoplasmic tail encoding amino acids 221–342 (CD2vi), amino acids 221–306 (CD2vii) and amino acids 297–335 (CD2viii) were cloned in the pGBT9 vector and co-transformed into yeast strain Y190 with activation domain plasmids containing inserts isolated from the porcine macrophage library screen (SH3P7i, SH3P7ii or SH3P7iii) or control clones encoding SH3 domains (pNox, p85PI3K, Lck, Fyn). Calcineurin interaction with A238L protein was included as a positive control for the library clones and the interaction of p22-Phox with pNox for the panel clones (Miskin *et al.*, 1998). Expression of β-galactosidase was assayed to estimate the strength of the interaction between binding domain fusion proteins and activation domain fusion proteins. X indicates that there was no reporter gene expression detected, + indicates weak reporter gene expression, ++ indicates strong reporter gene expression and ND indicates that the assay was not carried out.

	CD2vct	CD2vi	CD2vii	CD2viii	A238L	p22-Phox
Library clones						
Grb2	+	+	X	+	X	ND
SH3P7i	+	+	X	X	X	ND
SH3P7ii	++	++	X	++	X	ND
SH3P7iii	++	++	X	++	X	ND
Calcineurin	X	X	X	X	++	ND
Panel clones						
pNox	X	X	X	X	ND	++
p85PI3K	X	X	X	X	ND	X
Lck	X	X	X	X	ND	X
Fyn	X	X	X	X	ND	X

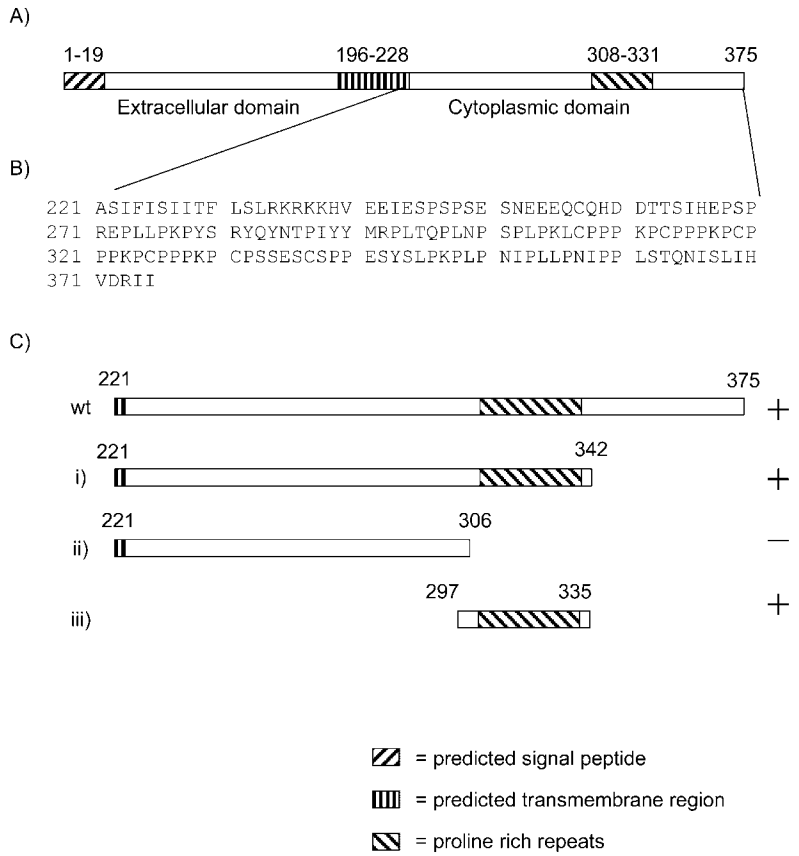

Fig. 3. Deletion mutants of the CD2v protein. (A) shows the structure of the complete CD2v protein from the Malawi LIL20/1 isolate. The positions of the predicted signal peptide, transmembrane domain and region containing proline-rich repeats are indicated. (B) shows the amino acid sequence of the predicted cytoplasmic domain. (C) shows the amino acid numbers included in the cytoplasmic tail and deletion mutants i, ii and iii of CD2v, which were used in yeast two-hybrid screens. Interactions of these deletion mutants with the SH3P7 protein as assayed using the yeast two-hybrid system are indicated with a positive or negative sign. These results are also shown in Table 1.

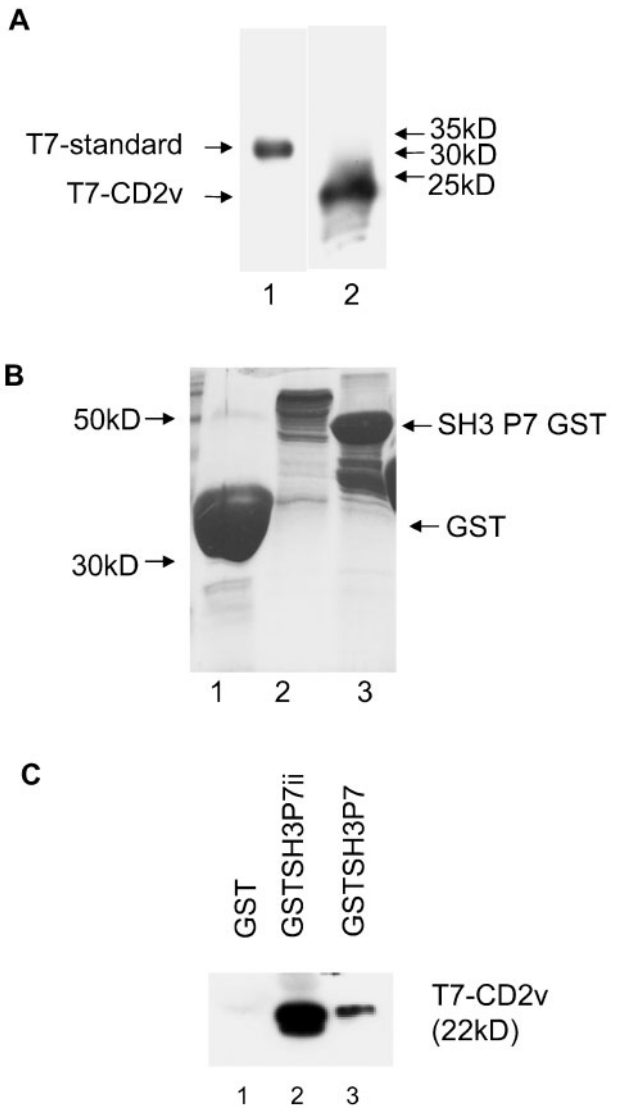

Fig. 4. *In vitro* binding of the cytoplasmic tail of CD2v to SH3P7 proteins. (A) shows a T7-tagged standard protein (lane 1) and the cytoplasmic tail of the CD2v protein fused to the T7 tag in the pET 21A vector (lane 2) and purified using anti-T7 antibody coupled to agarose beads. The proteins were detected by Western blotting of an SDS-PAGE gel followed by probing with an antibody that recognizes the T7 tag. (B) shows a Coomassie-stained SDS-PAGE gel on which purified GST (lane 1), GST fused to the complete SH3P7 protein from mouse (lane 2) and GST fused to the porcine SH3P7ii protein (GSTSH3P7ii) (lane 3) were loaded. In (C), GST (lane 1), the GSTSH3P7ii protein (lane 2) and GSTSH3P7 from mouse (lane 3) were mixed in equal quantities with T7CD2v protein. Proteins bound to GST fusion proteins were affinity purified using glutathione–Sepharose, washed twice with buffer containing 0·05 % deoxycholate, 0·5 % NP-40, 150 mM NaCl, 50 mM Tris/HCl, pH 7·5, and separated by SDS-PAGE, then blotted onto Hybond C membrane. T7CD2v protein was detected by probing with mouse monoclonal antibody that recognizes the T7 tag and HRP-conjugated goat anti-mouse secondary antibody, and bound antibodies were detected by ECL.

glutathione–Sepharose in 0·025 % NP-40 in PBS for 2 h at 4 °C. Bound proteins were washed three times in buffer containing NP-40 and NaCl, separated by SDS-PAGE and blotted onto nitrocellulose. T7CD2vct was detected by immunoblotting using the anti-T7 antibody (Fig. 4C). Strong binding of T7CD2vct to GSTSH3P7 and GSTSH3P7ii was detected at up to 1 % NP-40 and up to 500 mM NaCl (Fig. 4C, lanes 2 and 3, and data not shown). No binding of T7CD2vct to purified GST (Fig. 4C, lane 1) and no binding of a control T7 tagged protein (T7 α-NAC; Goatley *et al.*, 2002) to GSTSH3P7 or GSTSH3P7ii were detected (data not shown). These results show that the interaction between the CD2v cytoplasmic tail and SH3P7 is direct, specific and stable in high detergent and salt concentrations.

CD2v and SH3P7 co-localize in areas surrounding virus factories

To determine whether CD2v and SH3P7 co-localize in ASFV-infected cells, the full-length SH3P7 gene fused downstream from the EGFP gene was cloned under the control of the ASFV late promoter VP72. ASFV-infected Vero cells were transfected with this VP72GFPSH3P7 plasmid and the CD2vHA plasmid and fixed at various times post-infection. CD2vHA was detected using the anti-HA antibody, shown in red (Fig. 2). EGFPSH3P7 expression is shown in green. SH3P7 was concentrated in areas around the virus factory but was also at the cell periphery and elsewhere in the cytoplasm (Fig. 2B). Overlaid images showed that CD2vHA co-localized with EGFPSH3P7 around the virus factories (Fig. 2C). CD2vHA and EGFPSH3P7 showed similar distributions in ASFV-infected cells when transfected individually (Fig. 2D, and data not shown). Virus factories are indicated with an arrow (Fig. 2C, F and I) and were stained both with DAPI (Fig. 2C, F and I) and with a monoclonal antibody against the VP72 virus capsid protein (Fig. 2E, F and I).

SH3P7 co-localizes with actin filaments at membrane ruffles and in the periplasm (Larbolette *et al.*, 1999; Kessels *et al.*, 2000). SH3P7 also associates with the Golgi network (Warren *et al.*, 2002; Fucini *et al.*, 2002). To determine whether CD2vHA was present in membrane areas derived from the Golgi, we infected cells with the ASFV BA71V isolate and transfected them with the CD2vHA plasmid. Cells were fixed 16 h post-infection and stained with an antibody against a Golgi protein (Harrison-Lavoie *et al.*, 1993) (Fig. 2H, green) and with anti-HA antibody to detect CD2vHA (Fig. 2G, red). Virus factories were stained with DAPI (blue) and with a monoclonal antibody against the virus capsid protein VP72 (Fig. 2I, white). The anti-Golgi antibody stained the areas around the virus factories where CD2vHA was located. CD2vHA did not co-localize with this Golgi protein (Fig. 2I) suggesting that the proteins are in the same structures but do not interact. The Golgi distribution differed in ASFV-infected cells compared with uninfected cells, as previously described

(McCrossan *et al.*, 2001) (Fig. 2H). Uninfected cells did not express CD2vHA.

Sequence analysis and tissue-specific expression of porcine SH3P7

The inserts in clones SH3P7i, SH3P7ii and SH3P7iii isolated in the yeast two-hybrid screen were sequenced (Fig. 5). The SH3P7i clone encoded 93 amino acids of a protein with 90 % nucleotide identity and 83 % amino acid identity to the human SH3P7 sequence. The SH3 domain of SH3P7i comprised 59 amino acids with 98 % amino acid identity to the human SH3P7 SH3 domain. A tyrosine residue, which is phosphorylated in the mouse protein and also conserved in human, rat and mouse SH3P7 sequences, was present in SH3P7i.

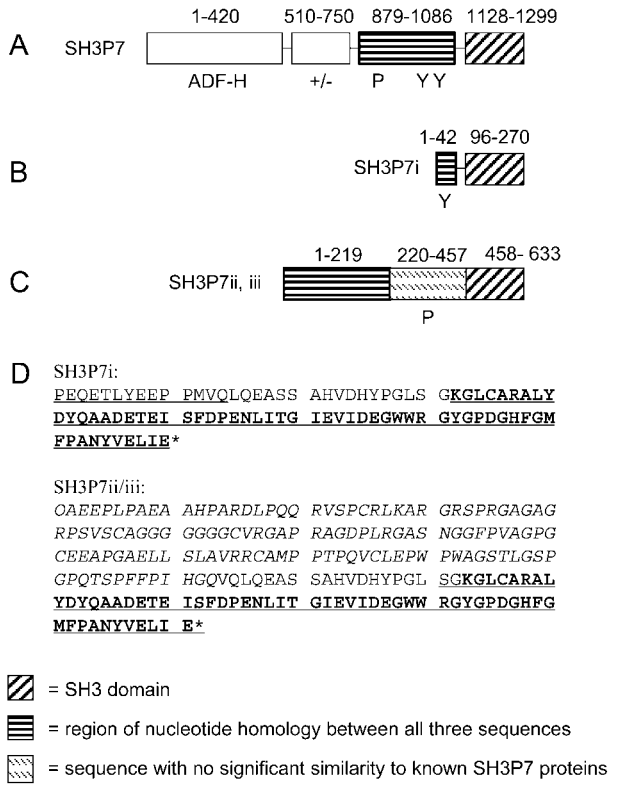

Fig. 5. Structure of clones encoding the SH3P7 protein. (A) shows the structure of the SH3P7 coding region. The nucleotide positions of the actin depolymerization-factor homology domain (ADF-H), highly charged domain (+/−) and SH3 domain are indicated. P shows the position of putative SH3 domain binding motifs and Y the position of putative tyrosine phosphorylation sites. (B) and (C) show the structure of the peptides encoded by clones SH3P7i, SH3P7ii and SH3P7iii, which were isolated in the two-hybrid screen with the CD2v cytoplasmic tail. The region encoding additional sequences with no similarity to other SH3P7 sequences is indicated. (D) shows amino acid sequences of proteins encoded by inserts in SH3P7i, -ii and -iii. Residues underlined are the same as in published sequences of SH3P7. The SH3 domain is shown in bold. The region encoded by SH3P7ii and -iii, which shares nucleotide similarity but no amino acid similarity to published SH3P7 sequences, is shown in italics.

The SH3P7ii and SH3P7iii clones contained inserts with the same 5′ start position, but the SH3P7iii clone contained an extra 50 nucleotides in the 3′ untranslated region. This shows that the two clones were independently isolated and thus likely to be genuine cDNA copies of mRNAs rather than generated by PCR or cloning artefacts. The nucleotide sequences of these inserts were similar to other SH3P7 genes over the first 219 nucleotides and over the SH3 domain between nt 457 and 633, but contained an extra 237 nucleotides between these regions. The proteins encoded by clones SH3P7ii and -iii have a different reading frame compared with the first 396 nucleotides from other SH3P7 sequences. A frame shift within the unique sequence in clones SH3P7ii and -iii means that the SH3 domain is read in the same reading frame as in other SH3P7 genes. Database searches with the predicted protein sequences of these variant clones, excluding the SH3 domain, identified no significant matches.

We used RACE PCR to clone the 5′ end of the porcine SH3P7 gene. RNA from porcine macrophages was reverse transcribed using primers that read from within the sequence from clones SH3P7ii and -iii towards the 5′ end of the gene. The cDNA was amplified by PCR using this primer and a primer that binds to the cap structure. The resulting fragment was cloned and sequenced. The predicted sequence of porcine SH3P7 was 430 amino acids long and shared 88 % and 83 % amino acid identity with the human and mouse proteins, respectively. The most variable regions of the protein were between residues 220 and 253 and residues 297 and 369 outside of the ADF-H and SH3 domains. We failed to obtain a full-length clone for the variant form of SH3P7 encoded by clones SH3P7ii and -iii.

To investigate porcine SH3P7 expression, we designed primers to amplify either the unique region in clones SH3P7ii and -iii or a conserved region of the gene from SH3P7 database sequences by RT-PCR. Fragments of the expected size ($\sim$230 bp for the variant sequence and $\sim$450 bp for the conserved sequence) were obtained from mRNA from a wide variety of tissues including brain, heart, muscle, liver and bone marrow (Fig. 6). Hybridization with a probe from the SH3P7 gene confirmed that these fragments contained SH3P7 sequences (data not shown). Smaller fragments amplified in some samples did not hybridize with the probe showing that they were non-specific (data not shown). These results suggest that the wild-type and variant forms of SH3P7 are expressed in a wide variety of porcine tissues. Poly(A)-containing RNA was used in these experiments, suggesting that these are mature mRNA sequences rather than primary transcripts. Previous analysis of mouse tissues showed that SH3P7 was expressed in B cells, testis, brain, heart, lung, thymus and spleen but not

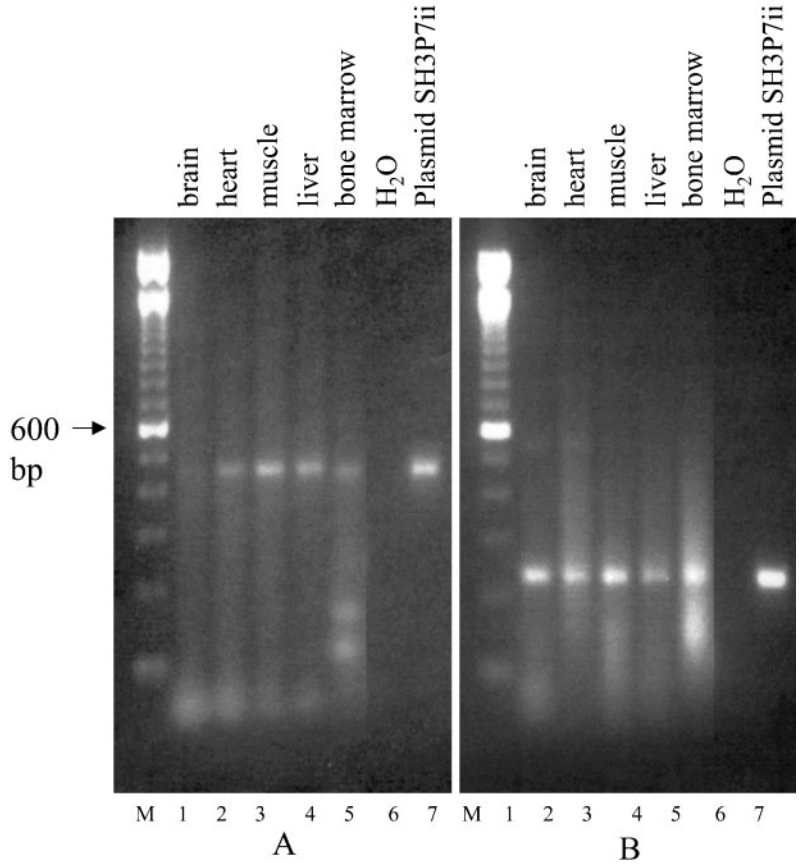

Fig. 6. RT-PCR of SH3P7 mRNAs from different porcine tissues. mRNA was isolated from different pig tissues. RT-PCR was used to amplify a conserved region of the SH3P7 gene (A) or the unique sequence present in the variant form of the SH3P7 gene present in clones SH3P7ii and SH3P7iii (B). The amplified products were analysed by electrophoresis on a 0·6 % agarose gel and compared with a 100 bp ladder (lane M). The plasmid containing the insert from SH3P7ii was used as a positive control (lane 7). Products amplified from brain (lane 1), heart (lane 2), muscle (lane 3), liver (lane 4) and bone marrow (lane 5) are shown.

muscle or ovary (Larbolette *et al.*, 1999). Human SH3P7 transcripts were found in all tissues tested including muscle (Ensenat *et al.*, 1999). Database searches identified SH3P7 cDNA sequences in many tissues including brain, mammary gland, thymus, gonad, eyeball, pituitary, bladder, bone, heart, lung and stomach.

DISCUSSION

We have shown that the cytoplasmic tail of the ASFV CD2v protein interacts with SH3P7, a protein involved in protein trafficking through the Golgi, endocytosis and signal transduction. We identified this interaction using the yeast two-hybrid system and confirmed it by direct binding using recombinant proteins. We have also shown, by confocal microscopy, that CD2v and SH3P7 co-localize in ASFV-infected cells in cytoplasmic areas surrounding virus factories, which derive from the Golgi network. SH3P7 is an adaptor protein with several functions. It contains an N-terminal ADF-H domain and a region enriched in charged amino acids. Its C terminus contains a putative SH3 domain recognition motif, two tyrosine phosphorylation sites and an SH3 domain (Larbolette *et al.*, 1999; Ensenat *et al.*, 1999; Kessels *et al.*, 2001). SH3P7 may be involved in lymphocyte activation by coupling the cytoplasmic tails of receptors to endocytic pathways and the actin cytoskeleton (Larbolette *et al.*, 1999; J. Wienands and others, unpublished results). SH3P7 binds to Huntington interacting protein 1R (HIP1R), which binds to clathrin-coated pits, implicating SH3P7 in endocytosis regulation. Functional analysis using an RNA interference approach showed that SH3P7 (mAbp1) is required for endocytosis but not lamellipodia formation (Mise-Omata *et al.*, 2003). Abp1, the yeast homologue of SH3P7, binds to the HIP1R yeast homologue, Sla2p, linking endocytosis in yeast to proteins regulating actin dynamics (Warren *et al.*, 2002). SH3P7 localizes at sites of F-actin formation, at areas of cell growth and at the leading edges of moving and spreading cells in a GTPase-dependent manner (Kessels *et al.*, 2000). In resting cells, it links the actin cytoskeleton to vesicle movement within the secretory pathway in the Golgi of fibroblasts and during synaptogenesis in neurons, again with GTPase regulation (Kessels *et al.*, 2001; Fucini *et al.*, 2002). SH3P7 may also have a role in the regulation of JNK1 signalling, leading to transcription factor activation (Ensenat *et al.*, 1999).

We observed co-localization of CD2v with SH3P7 around perinuclear virus factories in areas that were stained with an antibody to a Golgi protein. We also demonstrated that CD2v is partially resistant to endo-H digestion showing that it is transported beyond the endoplasmic reticulum, at least to the Golgi network. CD2v expression is required for the haemadsorption of erythrocytes around ASFV-infected cells, indicating that some CD2v is present at the cell surface. However, both our study and a previous study have

shown, using immunofluorescence, that most CD2v is inside cells (Ruiz-Gonzalvo & McColl, 1993). CD2v may either be retained within membrane compartments as it is transported to the cell surface, or may be retrieved to these compartments from the cell surface.

CD2v interacts with SH3P7 via an area of proline repeats. Binding is to the SH3 domain of SH3P7, since no other region is common to both the intact SH3P7 protein and the SH3P7ii variant, which both bind CD2v *in vitro*. SH3 domains contain two perpendicular β-sheets, forming a cleft, which the polyproline helices of their ligands fit into. The interaction is stabilized by a salt bridge at one end of the cleft between a basic residue in the ligand and an acidic residue in the SH3 domain. Ligands can bind along the cleft in either orientation: class I ligands have the basic residue at their N terminus and class II ligands at the C terminus (Yu *et al.*, 1994; Lim *et al.*, 1994; Feng *et al.*, 1994). SH3P7 was found in screens using class II ligands (Sparks *et al.*, 1996a, b). SH3 domains usually bind only to sets of related ligands (Feng *et al.*, 1994; Sparks *et al.*, 1996b). The class II consensus sequence, from the N to the C terminus, is X_3-P-p-X_2-P-p-X_1, where X_3 and X_2 are hydrophobic and X_1 is the stabilizing basic residue. P represents a critical proline, which interacts with the SH3 domain, and p represents a proline residue that maintains the structure of the polyproline II helix. The repeats in the CD2v protein consist of variable numbers of repeats of PCPPPK. As this sequence is repeated, the actual binding site may consist of a greater-than-unit-length sequence such as KPCPPPK, which is closest to the class II ligand consensus. The presence of repeated SH3 binding domains increases their local concentration and may make interactions with SH3 domains more likely (Feng *et al.*, 1994; Sparks *et al.*, 1996a). The SH3 domain of yeast Abp1 binds to unusual ligands containing two positive side-chains separated by seven or eight residues including a PXXP motif (Fazi *et al.*, 2002).

Several short polymorphisms within SH3P7 have been described, four from the rat protein and two from the mouse protein, apparently produced by alternative splicing. An additional putative SH3 domain binding motif is present in one rat isoform, but the functions of these forms are unknown (Yamazaki *et al.*, 2001; Kessels *et al.*, 2001). We identified two porcine SH3P7 homologues and showed that both are widely expressed in porcine tissues. The variant form of SH3P7 encodes the SH3 domain with an additional 237 bp and an upstream frame shift. The two phospho-tyrosine residues are not present (Larbolette *et al.*, 1999). A putative SH3 domain binding sequence is disrupted, but a new PXXP SH3 domain binding motif is introduced. The presence of motifs at the N terminus of this variant SH3P7, which we have not cloned and sequenced, cannot yet be determined. The function of this SH3P7 variant form is unknown, although the alterations in the variant form of domains involved in protein interactions are intriguing. A regulatory role in which the two forms of SH3P7 compete for ligand binding seems possible.

CD2v has several functions. It is required for erythrocyte haemadsorption around ASFV-infected cells and for adsorption of ASFV particles to the surface of erythrocytes. These properties may be important for virus dissemination around the host (Rodriguez *et al.*, 1993; Borca *et al.*, 1994; Wardley & Wilkinson, 1977; Thomson *et al.*, 1979; Borca *et al.*, 1998). CD2v also has an immunomodulatory role. ASFV infection of mononuclear cells greatly reduces the mitogen-dependent proliferation of uninfected lymphocytes, and expression of CD2v is required for this inhibition (Borca *et al.*, 1998). The interaction of CD2v with SH3P7 may be related to these effects, or to an uncharacterized function. The link between SH3P7 and JNK1 signalling could be involved in these immunomodulatory effects, via changes in transcription. Alternatively the interaction of CD2v with SH3P7 may modulate protein trafficking resulting in the inhibition of protein transport through the Golgi network to the cell surface, or modulation of endocytosis could affect the internalization of cell-surface molecules. Many virus-encoded proteins subvert host defence systems by altering receptor trafficking. Alterations in protein trafficking could alter signals delivered by infected macrophages to bystander lymphocytes. Actin filaments and the Golgi are rearranged in ASFV-infected cells (Carvalho *et al.*, 1988; Ferreira, 1996; Esteves *et al.*, 1986; McCrossan *et al.*, 2001) and SH3P7 could be involved in these rearrangements as it is linked to dynamic actin and to Golgi vesicles in other cell types. However, CD2v is non-essential for virus replication and any effects of its interaction with SH3P7 must therefore also not be required. The functions of SH3P7 and CD2v in ASFV-infected macrophages remain to be determined, but may provide insights into many aspects of ASFV replication and macrophage function.

ACKNOWLEDGEMENTS

We thank Dr Paul Monaghan and Pippa Hawes for confocal microscopy, and the BBSRC, DEFRA and EU project QLK3-CT-2000-00362 for funding. J. W. is supported by the Deutsche Forschungsgemeinschaft through SFB549 and EU IMPAC program QLG1-CT-2001-01536.

REFERENCES

Bierer, B. E., Peterson, A., Gorga, J. C., Herrmann, S. H. & Burakoff, S. J. (1988). Synergistic T cell activation via the physiological ligands for CD2 and the T cell receptor. *J Exp Med* **168**, 1145–1156.

Borca, M. V., Kutish, G. F., Afonso, C. L., Irusta, P., Carrillo, C., Brun, A., Sussman, M. & Rock, D. L. (1994). An African swine fever virus gene with similarity to the T-lymphocyte surface antigen CD2 mediates hemadsorption. *Virology* **199**, 463–468.

Borca, M. V., Carrillo, C., Zsak, L., Laegreid, W. W., Kutish, G. F., Neilan, J. G., Burrage, T. G. & Rock, D. L. (1998). Deletion of a CD2-like gene, 8-DR, from African swine fever virus affects viral infection in domestic swine. *J Virol* **72**, 2881–2889.

Brun, A., Rodriguez, F., Escribano, J. M. & Alonso, C. (1998). Functionality and cell anchorage dependence of the African swine fever virus gene A179L, a viral bcl-2 homolog, in insect cells. *J Virol* **72**, 10227–10233.

Carvalho, Z. G., De Matos, A. P. & Rodrigues-Pousada, C. (1988). Association of African swine fever virus with the cytoskeleton. *Virus Res* **11**, 175–192.

Cobbold, C., Whittle, J. T. & Wileman, T. (1996). Involvement of the endoplasmic reticulum in the assembly and envelopment of African swine fever virus. *J Virol* **70**, 8382–8390.

Dixon, L. K. (1988). Molecular cloning and restriction enzyme mapping of an African swine fever virus isolate from Malawi. *J Gen Virol* **69**, 1683–1694.

Dixon, L. K., Twigg, S. R., Baylis, S. A., Vydelingum, S., Bristow, C., Hammond, J. M. & Smith, G. L. (1994). Nucleotide sequence of a 55 kbp region from the right end of the genome of a pathogenic African swine fever virus isolate (Malawi LIL20/1). *J Gen Virol* **75**, 1655–1684.

Dixon, L. K., Costa, J. V., Escribano, J. M., Rock, D. L., Vinuela, E. & Wilkinson, P. J. (2000). The *Asfarviridae*. In *Virus Taxonomy. Seventh Report of the International Committee on Taxonomy of Viruses*, pp. 150–165. Edited by M. H. V. van Regenmortel, C. M. Fauquet, D. H. L. Bishop, E. B. Carstens, M. K. Estes, S. M. Lemon, J. Maniloff, M. A. Mayo, D. J. McGeoch, C. R. Pringle & R. B. Wickner. San Diego: Academic Press.

Dustin, M. L., Olszowy, M. W., Holdorf, A. D. & 8 other authors (1998). A novel adaptor protein orchestrates receptor patterning and cytoskeletal polarity in T-cell contacts. *Cell* **94**, 667–677.

Ensenat, D., Yao, Z., Wang, X. S., Kori, R., Zhou, G., Lee, S. C. & Tan, T. H. (1999). A novel src homology 3 domain-containing adaptor protein, HIP-55, that interacts with hematopoietic progenitor kinase 1. *J Biol Chem* **274**, 33945–33950.

Esteves, A., Marques, M. I. & Costa, J. V. (1986). Two-dimensional analysis of African swine fever virus proteins and proteins induced in infected cells. *Virology* **152**, 192–206.

Estojak, J., Brent, R. & Golemis, E. A. (1995). Correlation of two-hybrid affinity data with in vitro measurements. *Mol Cell Biol* **15**, 5820–5829.

Fazi, B., Cope, J. T. V., Douangamath, A. & 7 other authors (2002). Unusual binding properties of the SH3 domain of the yeast actin-binding protein Abp1: structural and functional analysis. *J Biol Chem* **277**, 5290–5298.

Feng, S., Chen, J. K., Yu, H., Simon, J. A. & Schreiber, S. L. (1994). Two binding orientations for peptides to the Src SH3 domain: development of a general model for SH3–ligand interactions. *Science* **266**, 1241–1247.

Ferreira, C. (1996). Expression of ubiquitin, actin, and actin-like genes in African swine fever virus infected cells. *Virus Res* **44**, 11–21.

Fucini, R. V., Chen, J. L., Sharma, C., Kessels, M. M. & Stamnes, M. (2002). Golgi vesicle proteins are linked to the assembly of an actin complex defined by mAbp1. *Mol Biol Cell* **13**, 621–631.

Goatley, L. C., Twigg, S. R., Miskin, J. E., Monaghan, P., St-Arnaud, R., Smith, G. L. & Dixon, L. K. (2002). The African swine fever virus protein j4R binds to the alpha chain of nascent polypeptide-associated complex. *J Virol* **76**, 9991–9999.

Harrison-Lavoie, K. J., Lewis, V. A., Hynes, G. M., Collison, K. S., Nutland, E. & Willison, K. R. (1993). A 102 kDa subunit of a Golgi-associated particle has homology to beta subunits of trimeric G proteins. *EMBO J* **12**, 2847–2853.

Kessels, M. M., Engqvist-Goldstein, A. E. & Drubin, D. G. (2000). Association of mouse actin-binding protein 1 (mAbp1/SH3P7), an Src kinase target, with dynamic regions of the cortical actin cytoskeleton in response to Rac1 activation. *Mol Biol Cell* **11**, 393–412.

Kessels, M. M., Engqvist-Goldstein, A. E., Drubin, D. G. & Qualmann, B. (2001). Mammalian Abp1, a signal-responsive F-actin-binding protein, links the actin cytoskeleton to endocytosis via the GTPase dynamin. *J Cell Biol* **153**, 351–366.

Kirsch, K. H., Georgescu, M. M., Ishimaru, S. & Hanafusa, H. (1999). CMS: an adapter molecule involved in cytoskeletal rearrangements. *Proc Natl Acad Sci U S A* **96**, 6211–6216.

Lappalainen, P., Kessels, M. M., Cope, M. J. & Drubin, D. G. (1998). The ADF homology (ADF-H) domain: a highly exploited actin-binding module. *Mol Biol Cell* **9**, 1951–1959.

Larbolette, O., Wollscheid, B., Schweikert, J., Nielsen, P. J. & Wienands, J. (1999). SH3P7 is a cytoskeleton adapter protein and is coupled to signal transduction from lymphocyte antigen receptors. *Mol Cell Biol* **19**, 1539–1546.

Lim, W. A., Richards, F. M. & Fox, R. O. (1994). Structural determinants of peptide-binding orientation and of sequence specificity in SH3 domains. *Nature* **372**, 375–379.

McCrossan, M., Windsor, M., Ponnambalam, S., Armstrong, J. & Wileman, T. (2001). The trans Golgi network is lost from cells infected with African swine fever virus. *J Virol* **75**, 11755–11765.

Mayer, B. J. & Gupta, R. (1998). Functions of SH2 and SH3 domains. *Curr Top Microbiol Immunol* **228**, 1–22.

Mise-Omata, S., Montagne, B., Deckert, M., Wienands, J. & Acuto, O. (2003). Mammalian actin binding protein 1 is essential for endocytosis but not lamellipodia formation: functional analysis by RNA interference. *Biochem Biophys Res Commun* **301**, 704–710.

Miskin, J. E., Abrams, C. C., Goatley, L. C. & Dixon, L. K. (1998). A viral mechanism for inhibition of the cellular phosphatase calcineurin. *Science* **281**, 562–565.

Miskin, J. E., Abrams, C. C. & Dixon, L. K. (2000). African swine fever virus protein A238L interacts with the cellular phosphatase calcineurin via a binding domain similar to that of NFAT. *J Virol* **74**, 9412–9420.

Nogal, M. L., Buitrago, G. G., de Rodriguez, C., Cubelas, B., Carrascosa, A. L., Salas, M. L. & Revilla, Y. (2001). African swine fever virus IAP homologue inhibits caspase activation and promotes cell survival in mammalian cells. *J Virol* **75**, 2536–2543.

Pawson, T. (1995). Protein modules and signalling networks. *Nature* **373**, 573–580.

Pawson, T. & Schlessinger, J. (1993). SH2 and SH3 domains. *Curr Biol* **3**, 432–442.

Powell, P. P., Dixon, L. K. & Parkhouse, R. M. (1996). An IkappaB homolog encoded by African swine fever virus provides a novel mechanism for downregulation of proinflammatory cytokine responses in host macrophages. *J Virol* **70**, 8527–8533.

Revilla, Y., Cebrian, A., Baixeras, E., Martinez, C., Vinuela, E. & Salas, M. L. (1997). Inhibition of apoptosis by the African swine fever virus Bcl-2 homologue: role of the BH1 domain. *Virology* **228**, 400–404.

Revilla, Y., Callejo, M., Rodriguez, J. M., Culebras, E., Nogal, M. L., Salas, M. L., Vinuela, E. & Fresno, M. (1998). Inhibition of nuclear factor κB activation by a virus-encoded IκB-like protein. *J Biol Chem* **273**, 5405–5411.

Rodriguez, J. M., Yanez, R. J., Almazan, F., Vinuela, E. & Rodriguez, J. F. (1993). African swine fever virus encodes a CD2 homolog responsible for the adhesion of erythrocytes to infected cells. *J Virol* **67**, 5312–5320.

Ruiz-Gonzalvo, F. & McColl, J. M. (1993). Characterization of a soluble hemagglutinin induced in African swine fever virus-infected cells. *Virology* **218**, 285–289.

Selvaraj, P., Dustin, M. L., Mitnacht, R., Hunig, T., Springer, T. A. & Plunkett, M. L. (1987). Rosetting of human T lymphocytes with sheep and human erythrocytes. Comparison of human and sheep ligand binding using purified E receptor. *J Immunol* **139**, 2690–2695.

Sparks, A. B., Hoffman, N. G., McConnell, S. J., Fowlkes, D. M. & Kay, B. K. (1996a). Cloning of ligand targets: systematic isolation of SH3 domain-containing proteins. *Nat Biotechnol* **14**, 741–744.

Sparks, A. B., Rider, J. E., Hoffman, N. G., Fowlkes, D. M., Quillam, L. A. & Kay, B. K. (1996b). Distinct ligand preferences of Src homology 3 domains from Src, Yes, Abl, Cortactin, p53bp2, PLCgamma, Crk, and Grb2. *Proc Natl Acad Sci U S A* **93**, 1540–1544.

Thomson, G. R., Gainaru, M. D. & van Dellen, A. F. (1979). African swine fever: pathogenicity and immunogenicity of two non-haemadsorbing viruses. *Onderstepoort J Vet Res* **46**, 149–154.

Wardley, R. C. & Wilkinson, P. J. (1977). The association of African swine fever virus with blood components of infected pigs. *Arch Virol* **55**, 327–334.

Warren, D. T., Andrews, P. D., Gourlay, C. W. & Ayscough, K. R. (2002). Sla1p couples the yeast endocytic machinery to proteins regulating actin dynamics. *J Cell Sci* **115**, 1703–1715.

Yamazaki, H., Takahashi, H., Aoki, T. & Shirao, T. (2001). Molecular cloning and dendritic localization of rat SH3P7. *Eur J Neurosci* **14**, 998–1008.

Yanez, R. J., Rodriguez, J. M., Nogal, M. L., Yuste, L., Enriquez, C., Rodriguez, J. F. & Vinuela, E. (1995). Analysis of the complete nucleotide sequence of African swine fever virus. *Virology* **208**, 249–278.

Yozawa, T., Kutish, G. F., Afonso, C. L., Lu, Z. & Rock, D. L. (1994). Two novel multigene families, 530 and 300, in the terminal variable regions of African swine fever virus genome. *Virology* **202**, 997–1002.

Yu, H., Chen, J. K., Feng, S., Dalgarno, D. C., Brauer, A. W. & Schreiber, S. L. (1994). Structural basis for the binding of proline-rich peptides to SH3 domains. *Cell* **76**, 933–945.